Photoaligned Nanorod Enhancement Films with Polarized Emission for Liquid-Crystal-Display Applications

Abhishek K. Srivastava, Wanlong Zhang, Julian Schneider, Andrey L. Rogach,* Vladimir G. Chigrinov, and Hoi-Sing Kwok*

Semiconductor nanorods (NR) emit polarized light, which is expected to bring manifold benefits, in terms of brightness and color enhancement, for modern liquid-crystal displays (LCD). In this regard, photoaligned nanorod enhancement films (NREF) for color and polarization conversion for LCD backlights are introduced here. The photoinduced anchoring forces, by the photoalignment layer, stimulate well-ordered self-assembly of NR in the thin polymer films. Green and red emitting NR with a quantum yield of ≈80% are aligned unidirectionally and in-plane, showing a polarization ratio of >7:1 and a degree of polarization of >0.81. The photoalignment technique facilitates the fabrication of mixed and multiple stacked NREF for LCDs, which improves the color gamut and polarization efficiency, and is thus expected to increase the optical efficiency of conventional LCDs by ≈60%.

Recently, quantum dot enhancement films (QDEF) have been widely explored for display backlight applications and have become increasingly popular in modern liquid crystal displays (LCD).[1] QDEF consist of green and red emitting semiconductor nanocrystals termed quantum dots (QD), which are dispersed in a polymer film. The QDEF works as a photoconversion layer that absorbs blue light and emits green and red light with narrow bandwidth, thus improving the color gamut of modern LCD to >100% of the NTSC color triangle.[1,2] Furthermore, because of the narrow emission bandwidth of QD, QDEF enable to match the backlight spectrum perfectly to the color filter bandwidths, which also improves the optical efficiency.[2] Materials that have been used in this regard include CdSe and InP-based core–shell QD,[1b,2,3] as well as perovskite nanocrystals.[4] Apart from spherical QD, prominent alternatives include 2D nanoplatelets,[5] and especially rod-shaped nanocrystals, termed nanorods (NR). Due to their polarized emission, NR possess great potential to improve LCD backlight units (BLU) in terms of the overall optical efficiency. **Table 1** compares the efficiency of a conventional LCD with a LCD equipped with polarized light emitters (i.e. NREF) as a color conversion layer for the BLU. The LCD structure shown in **Figure 1**a is characterized by an overall optical efficiency of around 3–5%.[6] The color filters and polarizers are the two main LCD components responsible for the light loss of more than 70%. The concept of field sequential color display was introduced to manage the losses of color filters, but finding solutions to increase the polarization efficiency of modern LCD still imposes a challenge.[7] A comparative analysis of the component-wise optical efficiency for the LCD as shown in Table 1, which gives <5% final image brightness, confirms that use of NREF, with a degree of polarization (DOP) of ≈0.7, increases the polarization efficiency of the polarizer films from 45% to 70%, and therefore, the overall efficiency of the conventional LCDs may increase from 3–5% to 6–8% for LCD with a NREF.

A high DOP has been observed for the emitted light along the wurtzite *c*-axis of semiconductor NR.[8] This phenomenon was explained by the fine structure splitting of the band-edge exciton and a crossing of the highest energy levels at NR aspect ratios (AR) larger than 1.2:1.[8f,9] Due to the shape dependence of the electronic level structure, the DOP grows with the increasing AR of NR and increases further by the anisotropic dielectric environment (Figure 1b).[8b,f] While core-only CdSe NR are able to emit linearly polarized light, their low photoluminescence quantum yield (PL QY) limits their use in displays. Core–shell NR, such as CdSe/CdS, show both high PL QY and high DOP.[10] The DOP for heterostructured nanocrystals, e.g., CdSe/CdS dot-in-rod structures such as illustrated in Figure 1b, also depends on the shell thickness along the shorter side, which affects the local anisotropy of the core material.[9,11] Additionally, the dipolar emission of the NR offers higher output light coupling in comparison to QD, as illustrated in Figure 1c,d.[12] Thus, it is expected that the aligned NR films, provided they possess high-order parameter and large-scale uniformity, would emit polarized light with high DOP and, therefore, further enhance the efficiency of the LCD in comparison with QDEF technology.

The alignment of NR with high-order parameter is critically important, and several techniques have been explored in this regard, viz., evaporation-mediated assembly,[13] electric field-assisted assembly,[14] template-assisted assembly,[15] chemical

Prof. A. K. Srivastava, W. Zhang, Prof. V. G. Chigrinov, Prof. H.-S. Kwok
State Key Laboratory on Advanced Displays and Optoelectronics Technologies
Department of Electronic and Computer Engineering
Hong Kong University of Science and Technology
Clear Water Bay, Kowloon, Hong Kong
E-mail: eeabhishek@ust.hk

J. Schneider, Prof. A. L. Rogach
Department of Physics and Materials Science and Centre for Functional Photonics (CFP)
City University of Hong Kong
83 Tat Chee Avenue, Kowloon, Hong Kong
E-mail: andrey.rogach@cityu.edu.hk

DOI: 10.1002/adma.201701091

Table 1. LCD components with their optical efficiencies and brightnesses, compared for conventional LCD with QDEF and for LCD with NREF.

	Components	Efficiency and Brightness of the LCD			
		Conventional LCD with QDEF		LCD with NREF	
		Efficiency [%]	Brightness [%]	Efficiency [%]	Brightness [%]
1	Backlight	100.0	100.0	100.0	100.0
2	Light diffusive films	75.0	75.0	75.0	75.0
3	Polarizers	45.0	33.8	70.0	52.5
4	Glass	95.0	32.1	95.0	49.9
5	TFT active matrix	65.0	20.8	65.0	32.4
6	LC matrix	85.0	17.7	85.0	27.6
7	Glass	95.0	16.8	95.0	26.2
8	Color Filter	30.0	5.0	30.0	8.3
9	Analyzer	95.0	4.8	95.0	7.9
	Final Image		4.8	→	7.9
	Color Triangle		>100 NTSC		>100 NTSC

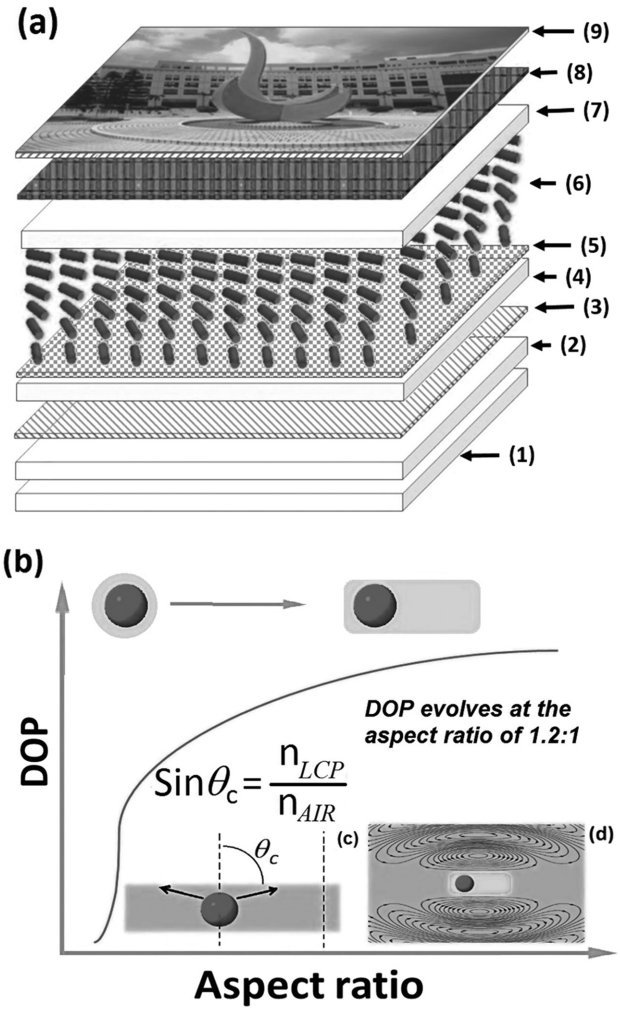

Figure 1. a) The common LCD architecture including: 1) BLU, 2) optical film, 3) polarizer, 4,7) glass substrates, 5) thin-film transistor (TFT) active matrix, 6) liquid-crystal layer, 8) color filter, and 9) the analyzer. b) Schematics of the evolution of the DOP with the shape of the emitting dot- and rod-shaped nanostructures, c,d) The emissions from dots and rods are represented, wherein the emissions from the dots have limitations of total internal reflection angle shown by the equation above the scheme, while rods provide better light coupling because of the dipolar emission.

bonding-directed self-assembly,[16] LC self-alignment,[17] Langmuir–Blodgett deposition,[18] mechanical rubbing,[19] and several more.[20] While most of these methods control the assembly of NR by an external force, they offer limited flexibility for the local alignment orientation, which reduces their prospects regarding large-scale fabrication, required for LCD. Electrospinning[21] and stretching of polymer films[5b] have recently showed significant advantages in this respect. The electrospinning utilizes a high electric field to fabricate nanofiber bundles, which contain NR. The composite nanofibers were collected by a high-speed rotating disk and drum, producing large sheets. This approach resulted in highly uniform NR films; however, high electric fields and the complicated fabrication process are the hurdles to overcome. On the other hand, the stretched film approach, illustrated by Cunningham et al., offers simplicity and good uniformity, but significant stretching is required, which is challenging for larger scale fabrication.[5b] Furthermore, both of these approaches, in addition to many others, provide 3D NR distribution with poor in-plane control, which limits the highest reported DOP to 0.64 for CdSe/CdS dot-in-rod nanostructures.[5b,13–21] Theoretically, the maximum DOP can be achieved for NR, which are uniformly aligned in-plane (i.e., the zero pretilt angle such as shown in **Figure 2**a) with high-order parameter.

Photoalignment technology is known to offer alignment characteristics, such as a zero pretilt angle and high anchoring energy for the planar alignment of liquid crystals and liquid crystal polymers (LCP), with precise control at the nanoscale. There are four photoalignment mechanisms, namely, i) anisotropic photodegradation,[22] ii) anisotropic photo-crosslinking,[23] iii) *cis–trans* isomerization,[24] and iv) the photo-reorientation of the chromophores.[25] In our previous work,[26] it was shown that photo-reorientation of chromophores is the most suitable for the purpose of NR alignment since it offers large anchoring energy (≈10^{-3} J m^{-2}) with high in-plane easy axis control, i.e., the small pretilt angle (<0.2°).[25–27] The strategy provides high spatial-alignment resolution[26b,27a] and facilitates NR alignment in LCP, achieving a NR order parameter of 0.87 and a DOP of 0.62.[26a]

Here, we demonstrate the superior character of photoalignment in terms of the fabrication of NREF with polarized emission, based on two species of red and green emitting NR, as shown in Figure 2. Highly emissive CdSe/CdS core–shell NRs were synthesized by a hot-injection seeded growth approach in the coordinating solvents trioctylphosphine and trioctylphosphine oxide, using a mixture of ligands with long alkyl chains, namely, octadecylphosphonic acid and hexylphosphonic acid.[28] The UV–vis absorption spectra in Figure 2b show the characteristic contributions from the CdSe core at 544 and 608 nm for the green and red emitting NR, respectively. The strong

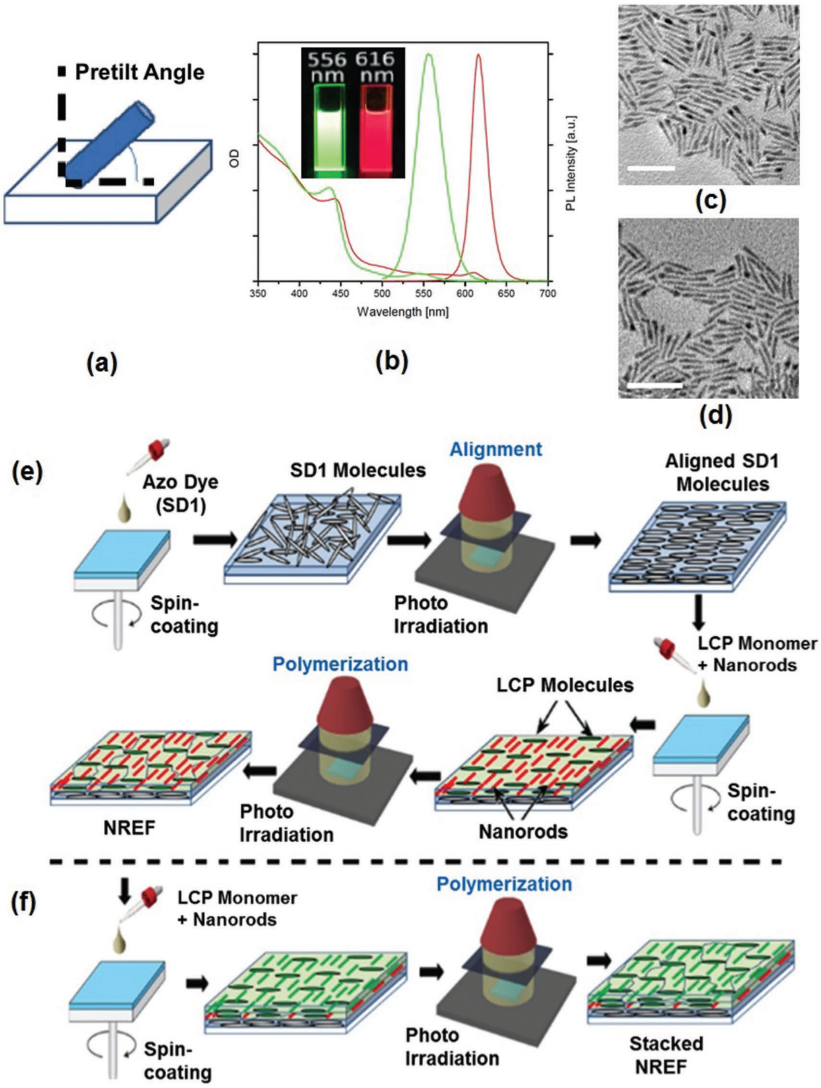

Figure 2. a) Schematic of the pretilt of NR from the substrate plan. b) Absorption and emission spectra of the red (red lines) and green (green lines) emitting CdSe/CdS NR, employed for the NREF fabrication. The inset shows photographs of NR solutions in toluene under UV exposure and the corresponding emission wavelengths. c,d) TEM images of the red and green NR, respectively. Scale bars are 50 nm. e) The processing flow of the photoalignment of the NR in the LCP films. f) The bottom section reveals the process to produce the multiple-layer NREF with same or different NR.

absorption signals at around 450 nm in both materials originate from the elongated CdS shells. Both NR species demonstrate strong excitonic emission at 556 and 616 nm with PL QY of 82% and 80%, and a spectral bandwidth of 39 and 24 nm, respectively (Figure 2b). The transmission electron microscopy (TEM) images in Figure 2c,d show the dimensions of both NR. Red emitting NR are 29.8 ± 2.5 nm in length, 4.1 ± 0.4 nm in width, and have an AR of 7:1. Green emitting NR have a length of 22.1 ± 2.1 nm, a width of 3.6 ± 0.3 nm, and an AR of 6:1.

The sulfonic azo dye tetrasodium5,5′-((1E,1′E)-(2,2′-disulfonato-[1,1′-biphenyl]-4,4′-diyl)bis(diazene-2,1-diyl))bis(2-hydroxybenzoate) (SD1), which operates under the fourth class of photoalignment mechanisms mentioned above, has been chosen as an alignment layer.[29] When the SD1 layer is irradiated by a polarized light of wavelength 450 nm, the energy absorbed by SD1 molecules is proportional to $\cos^2\theta$, where θ is the angle between the absorption oscillator of the dye and the *E*-vector of the irradiating light.[25] Therefore, the azo-dye molecules that have their transition dipole moments parallel to the *E*-vector of the impinging light receive excess energy, which results in their reorientation from the initial position to the direction orthogonal to the *E*-vector of the irradiating light. Thus, the polarized light exposure of the SD1 defines an alignment direction (i.e., easy axis) perpendicular to the *E*-vector of the irradiating light, with almost zero pretilt angle and high anchoring energy.[29] The anchoring energy of SD1 increases with the irradiation energy and saturates at higher energy doses.[27a,30]

The NREF fabrication is a multistep, yet straightforward and easily up-scalable, process shown in Figure 2e. It consists of spin coating and subsequent photoalignment of SD1 followed by spin coating a mixture of NR and LCP monomer in toluene, which is polymerized by UV light to ensure the long-term stability of the resulting composite films. Figure 2f introduces the ability to align multiple stacked layers of NREF, which highlights the versatile character of the method. The photoinduced anisotropic surface energy of the SD1 alignment layer transfers a torque to the LCP molecules and aligns them in a direction parallel to the easy axis of the SD1.[25,27b] Simultaneously, repulsive intermolecular forces between the NR ligands and LCP molecules, which exert counter-torque on NR, align NR perpendicular to the easy axis of the SD1. The NR ligands, to minimize the energy, try to fit in the monomer matrix like a comb, and thus provide a long-range order to NR.[26a] In our previous work, the order parameter of the NREF was calculated from the TEM images and found to be ≈0.87, wherein more than 70% of NRs are aligned in the cone angle of 10° from the alignment directions.[26a]

The NREF containing only one type of NR have been fabricated according to Figure 2e and characterized for their uniformity and polarized emission in **Figure 3**. The fluorescence microscopy images of the green- and red-emitting NREF are shown in Figure 3a(i),(ii), respectively, and confirm the microscopically uniform distribution of NR without any manifestation of clustering. TEM is the most reliable tool to characterize the order parameter of the NR alignment, but it demands a film thickness <100 nm. In the present case, the film thickness, to maintain the sufficiently high brightness (≈99 nits), was ≈700 nm, and therefore, it was not easy to retrieve any vital information about the NR alignment by TEM. With dark-field TEM imaging (Figure 3b) however, it was possible to observe

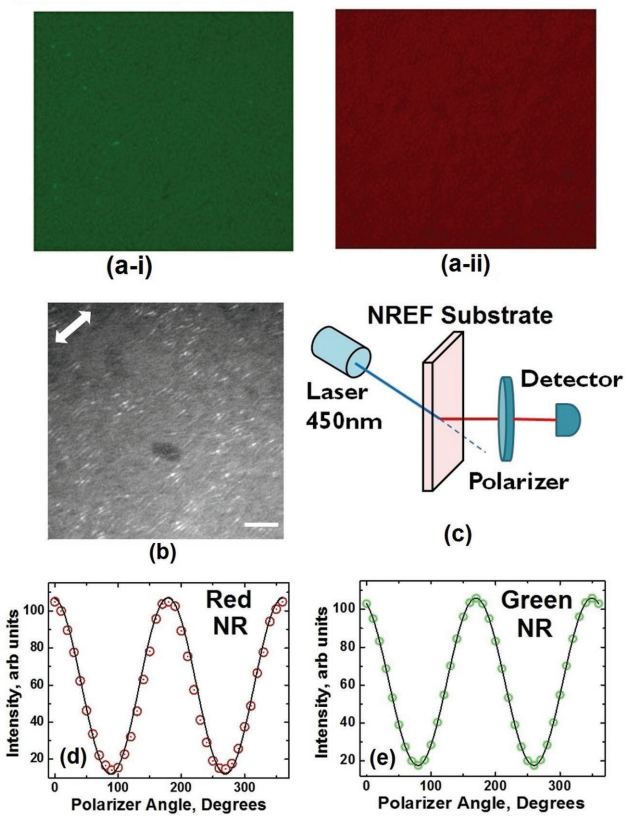

Figure 3. a) 250 µm × 250 µm fluorescence microscopy images for green (i) and red (ii) emitting NREF. b) TEM image of the single NREF with the film thickness of 700 nm, the white arrow denotes the alignment direction of NR, and the scale bar is 100 nm. c) Optical setup to measure the DOP. The corresponding curves for the emission intensity as a function of the polarizer axis rotation angle are presented in d) for red NREF and e) for green NREF.

NR with high-order parameter, where more than 70% of the NR were aligned in one direction illustrated by the white arrow.

To assess the polarization ratio and DOP, the experimental setup as presented in Figure 3c has been used. The polarization angle dependences of the emitted light for green and red NREF are presented in Figure 3d,e, respectively, and show good agreement with the Malus's law $I(\theta) = (I_{max} - I_{min})\cos^2\theta + I_{min}$.[31] The black line for the Malus's law fits well with the experimental data represented by the open circles for both red and green emitting NR. The measured polarization ratios (I_{max}/I_{min}) for the aligned red and green NREF are 7.8:1 and 7:1, respectively, which again confirms the high-quality alignment of NR in the NREF. The DOP, for the emitted light (defined as DOP = $(I_{max} - I_{min})/(I_{max} + I_{min})$), is measured as 0.83 and 0.81 for the aligned red and green NR, respectively. Such high DOP are characteristic for the dot-in-rod CdSe/CdS structures such as NR used here.[9,11,32] Thus, we have achieved NREF with both high DOP and large-scale uniformity. In the next step, optical characteristics of the aligned NREF for LCD BLU application are studied.

The NR in an NREF for the LCD backlights have to be arranged in a suitable configuration to provide the desired white balance of the BLU. There are two possible alternatives, first, mix both types of NR in the same film and optimize the concentration. In this configuration, it is particularly important for the green emitting NR to compensate the reabsorption of the green emission by the low-energy-emitting NR, i.e., red NR. Second, make a multiple-layer stack and arrange the high-energy emitters on the top of the low-energy emitters, which is a process flow illustrated in Figure 2f. It has been observed that the LCP layer coated on the top of the previously deposited photoalignment layer offers similar anchoring and alignment conditions that transfer all the local microscopic information to the subsequent LCP layers coated on the top of it, without any screening in the anchoring energy up to 2–3 layers.[33] Usually, alignment anchoring screening can be only observed after three stacked layers of LCP. Likewise, the NR/LCP composite film follows the same trend. The results for the NR aligned in multiple layers are shown in **Figure 4**. Figure 4a(i),(ii) present the mixed and multiple-layer NREF, illuminated by blue light. Both of these NREF show good white balance, uniformity, and high DOP. The emission intensities from these two films have been plotted against the polarizer rotation angle in Figure 4c,d, respectively. The DOP for the mixed NREF and multiple-layer NREF are measured as 0.67 and 0.76, respectively. Based on these results, one can conclude that photoalignment approach is suitable to align both NR in the same film with similar alignment quality. Second, NR can be aligned in the two stacked layers one over each other without compromising the alignment and optical quality. The small drop in the DOP for the multiple NREF (i.e., ≈0.76) in comparison to the single NREF (i.e., >0.8) can be attributed to small pretilt, screening in azimuthal anchoring for the second layer or mutual interaction between the NR and LCP in the two subsequently deposited layers. The multiple-layer NREF show higher DOP and lower fluorescence quenching, and therefore, we limited further studies only for the multiple-layer NREF. Furthermore, the NREF can be deposited by the same photoalignment technique on a flexible plastic substrate with the comparable optical quality, as shown in Figure 4b(i). Moreover, by simple process optimization, the NREF dimensions on the glass substrate have been extended from 4 to 25 cm^2, as shown in Figure 4b(ii).

The NREF introduced here rely on green and red polarized emitters, and therefore, all the benefits will be only for these two wavelengths; however, blue light has the same constraints of polarizers with polarization efficiency of ≈0.45. Furthermore, the blue light can also be absorbed by both kinds of these NR. These constraints are similar to the QDEF. Thus, to achieve the appropriate white balance, the intensity of the blue BLU and NR counts in the NREF should be optimized to achieve the equal intensity for all three wavelengths blue, green, and red. The PL spectra before and after the polarizer are shown in Figure 4e,f, respectively. With respect to the PL QY of the NR, and achieved DOP, the intensity of the blue light was set to be 1.5 times higher than the brightness of photoaligned NR, which after passing through the polarizer show equal intensities (Figure 4f).[34] There are two scaling factors for the NREF brightness. First, the PL QY of the NR, which for the present case was 82% for the green and 80% for the red NR. The second important factor is the DOP of the aligned NREF. The DOP for the photoaligned NREFs (i.e., >0.8), to the best of our knowledge, is very high in comparison to reported values,[5b,21] thus the PL

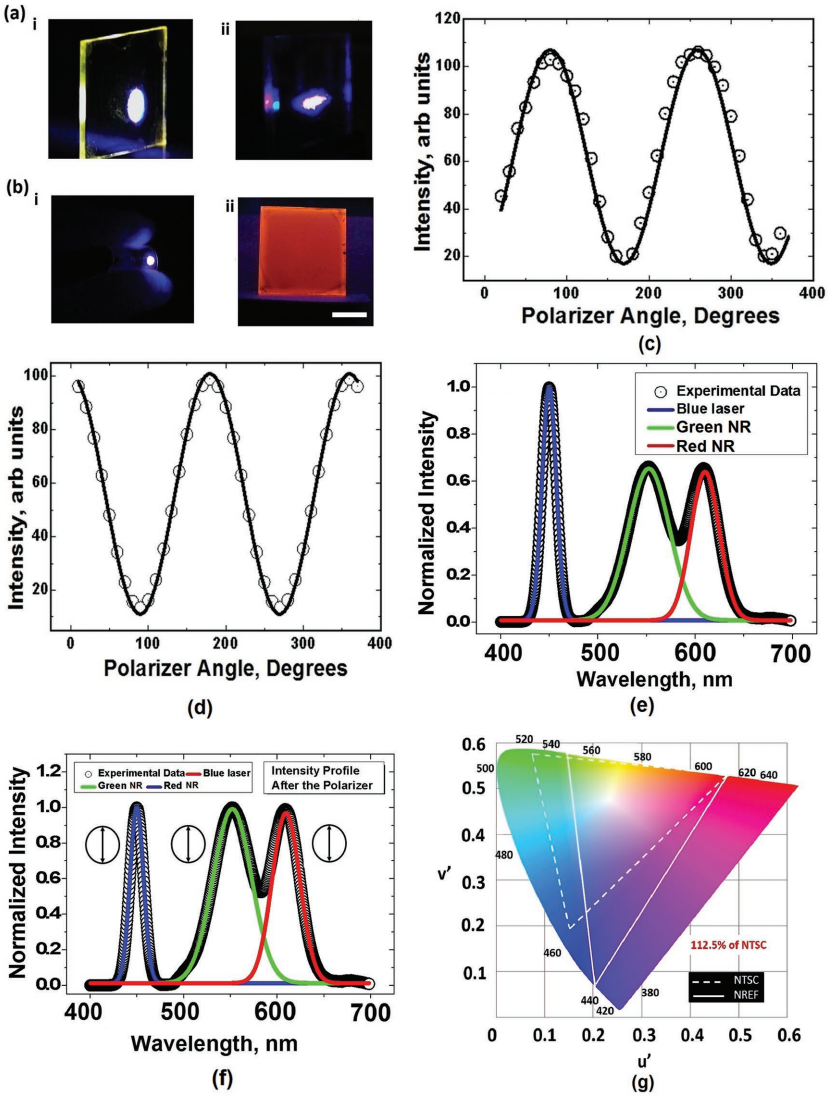

Figure 4. a) Photographs of specimens of NREF based on the mixed NR in a single layer (i), multiple layers with different NR in subsequently deposited films (ii). b) i) NREF on the plastic substrate, and ii) 5 cm × 5 cm NREF on glass (the scale bar is 2 cm). c,d) Intensity of the emitted light as a function of the polarizer axis rotation angle for the mixed NREF and the multiple-layer NREF, respectively. e) Experimental results for the multiple-layer NREF irradiated by the blue light that excites the NR for the light conversion. The open circles represent the spectral response of the NREF while illuminated with the blue light, whereas the color solid line shows the best fit to the respective color. f) The exciting blue light intensity was kept ≈3 times higher than the desired emission intensity, which, after passing through a polarizer, is comparable to the converted light intensity. The spectrum is shown in this part. g) The color performance of the NREF as compared with the NTSC standard in the CIE 1973 color space; NREF show better color performance than the NTSC.

QY is the limiting factor in the present case. The polarization efficiency for the NREF is equal to ≈57%, which is 27% higher than the conventional polarizers and improves the overall optical efficiency of the LCDs from 4.8% to 6.4% (see Table 1). Other than the polarization efficiency, the color performance of the NREF is another important parameter. The color triangle of the NREF is plotted in Figure 4g and shows that the narrow red emission of CdSe/CdS NR (Figure 2b) offers high color purity in the red spectral region, while somewhat broader emission of the NR in the green spectral region still holds some challenges. A narrower emission peak and shorter emission wavelength for the green emitters would help to enhance the color performance of the NREF, which can be achieved by further NR synthesis optimization or by employment of alternative nanomaterials with polarized emission such as CdSe-based nanoplatelets[5a,b] or perovskite nanocrystals.[4a,5c,35]

In summary, we have demonstrated photoaligned NREF for the brightness enhancement of the LCD. In addition to the color enhancement, the BLU equipped with NREF with a high-order parameter for the NR alignment and DOP for the polarized emission improves the polarization efficiency of the polarizer, resulting in a better optical efficiency of the LCD. The DOP of the NREF is measured as 0.83 and 0.81 for the aligned red and green NR, respectively, which to the best of knowledge are considerably higher than the reported values in the past. Furthermore, the DOP for mixed NREF and multiple-layer NREF is 0.67 and 0.76, respectively, which offers 33% higher brightness for the LCD. We achieved a brightness of 99 nits for the multiple-layer NREF, which can be further optimized for the different applications. The PL QY of NR appears to be the limiting factor for the LCD efficiency; however, it can be improved by the growth of a secondary shell on core–shell NR, as recently proposed.[10] Our photoalignment approach constitutes a straightforward, easily up-scalable fabrication, which is fully compatible with the roll-to-roll printing process, hence offering a useful way to fabricate NREF for application in modern LCD.

Experimental Section

Synthesis of CdSe/CdS Nanorods: In an adapted procedure from Carbone et al.,[28] CdSe/CdS core–shell NR were synthesized in two consecutive steps. To obtain CdSe seeds, TOP-Se was injected into a deaerated mixture of cadmium oxide, trioctylphosphine oxide, and octadecyl phosphonic acid at 340 °C. Depending on the intended size of the nanocrystals, the reaction was stopped after the different growth times. The CdSe seeds were washed multiple times by precipitation with methanol and dissolved in toluene. For the synthesis of the shell, the seeds were combined with TOP-S directly before the addition to the cadmium–ligand mixture at 350 °C. The resulting core–shell CdSe/CdS NR were repeatedly washed by a dissolution/precipitation procedure using toluene and methanol, to remove excess of the coordinating solvents.

Photoalignment Process: The process flow of the approach is shown in Figure 2e,f, wherein a solution of sulfonic azo dye (SD1 (purity > 98%) was provided by Dainippon Ink and Chemicals Ltd., Japan (DIC)) in dimethylformamide (2 wt%) is deposited on a glass substrate by spin

coating. After heating the substrate for 5 min to remove the excessive solvent, the irradiation of the SD1 layer by polarized light (λ = 450 nm and intensity 1.3 mW cm^{-2}) results in reorientation of the SD1 easy axis perpendicular to the *E*-vector of the irradiating light. For the hybrid NR/LCP film, NR and commercially available LCP (purity >97%, UCL017 from DIC) were dispersed in toluene, and the clear solution (0.24 µm NR/10 wt% LCP) was spin-coated on top of the pre-aligned SD1 layer.

Characterization: Optical characterization was conducted on a Varian Cary 50 UV–vis spectrophotometer and a Cary Eclipse photoluminescence spectrometer. TEM images were recorded on a Philips CM-20 electron microscope. A Leica DMI6000B was used to obtain fluorescence microscopy images. After the fabrication of the films, the DOP was recorded using an Ocean Optics spectrometer.

Acknowledgements

This work was supported by Hong Kong Government ITC grant No. ITS/370/16, by The State Key Laboratory on Advanced Displays and Optoelectronics Technologies, ECE Department, Hong Kong University of Science and Technology, Hong Kong, and by a grant from the Germany/Hong Kong Joint Research Scheme sponsored by the Research Grant Council of Hong Kong and the Germany Academic Exchange Service of Germany (Reference No.: G-CityU110/14).

Conflict of Interest

The authors declare no conflict of interest.

Keywords

liquid crystal display, liquid crystal polymer, photoalignment, polarized emission, semiconductor nanorods

Received: February 23, 2017
Revised: April 28, 2017
Published online: June 28, 2017

[1] a) S. Coe-Sullivan, *SID Symp. Dig. Tech. Pap.* **2016**, *47*, 239; b) E. Jang, S. Jun, H. Jang, J. Lim, B. Kim, Y. Kim, *Adv. Mater.* **2010**, *22*, 3076.
[2] Z. Luo, Y. Chen, S. T. Wu, *Opt. Express* **2013**, *21*, 26269.
[3] E. Mutlugun, P. L. Hernandez-Martinez, C. Eroglu, Y. Coskun, T. Erdem, V. K. Sharma, E. Unal, S. K. Panda, S. G. Hickey, N. Gaponik, A. Eychmuller, H. V. Demir, *Nano Lett.* **2012**, *12*, 3986.
[4] a) Q. Zhou, Z. Bai, W. G. Lu, Y. Wang, B. Zou, H. Zhong, *Adv. Mater.* **2016**, *28*, 9163; b) H. Huang, A. S. Susha, S. V. Kershaw, T. F. Hung, A. L. Rogach, *Adv. Sci.* **2015**, *2*.
[5] a) B. Abecassis, M. D. Tessier, P. Davidson, B. Dubertret, *Nano Lett.* **2014**, *14*, 710; b) P. D. Cunningham, J. B. Souza Jr., I. Fedin, C. She, B. Lee, D. V. Talapin, *ACS Nano* **2016**, *10*, 5769; c) L. Liu, S. Huang, L. Pan, L. J. Shi, B. Zou, L. Deng, H. Zhong, *Angew. Chem., Int. Ed.* **2017**, *56*, 1780.
[6] a) A. K. Srivastava, W. Zhang, J. Schneider, A. Susha, A. Rogach, V. G. Chigrinov, H. S. Kwok, *SID Symp. Dig. Tech. Pap.* **2016**, *47*, 602; b) V. G. Chigrinov, *Liquid Crystal Photonics*, Nova Science Publishers, Inc., Hauppauge, NY, USA **2014**.
[7] A. K. Srivastava, V. G. Chigrinov, H. S. Kwok, *J. Soc. Inf. Disp.* **2015**, *23*, 253.
[8] a) D. V. Talapin, R. Koeppe, S. Gotzinger, A. Kornowski, J. M. Lupton, A. L. Rogach, O. Benson, J. Feldmann, H. Weller, *Nano Lett.* **2003**, *3*, 1677; b) A. Shabaev, A. L. Efros, *Nano Lett.* **2004**, *4*, 1821; c) N. Le Thomas, E. Herz, O. Schops, U. Woggon, M. V. Artemyev, *Phys. Rev. Lett.* **2005**, *94*, 016803; d) Y. Louyer, L. Biadala, J. B. Trebbia, M. J. Fernee, P. Tamarat, B. Lounis, *Nano Lett.* **2011**, *11*, 4370; e) M. J. Fernee, C. Sinito, P. Tamarat, B. Lounis, *Nano Lett.* **2014**, *14*, 4480; f) J. Hu, L. Li, W. Yang, L. Manna, L. Wang, A. P. Alivisatos, *Science* **2001**, *292*, 2060.
[9] S. Vezzoli, M. Manceau, G. Lemenager, Q. Glorieux, E. Giacobino, L. Carbone, M. De Vittorio, A. Bramati, *ACS Nano* **2015**, *9*, 7992.
[10] I. Coropceanu, A. Rossinelli, J. R. Caram, F. S. Freyria, M. G. Bawendi, *ACS Nano* **2016**, *10*, 3295.
[11] B. T. Diroll, A. Koschitzky, C. B. Murray, *J. Phys. Chem. Lett.* **2014**, *5*, 85.
[12] a) E. Hecht, *Optics*, 5th ed., Pearson Education, Inc., Boston, MA, USA **2017**; b) F. Pisanello, L. Martiradonna, G. Lemenager, P. Spinicelli, A. Fiore, L. Manna, J. P. Hermier, R. Cingolani, E. Giacobino, M. De Vittorio, A. Bramati, *Appl. Phys. Lett.* **2010**, *96*, 033101.
[13] J. L. Baker, A. Widmer-Cooper, M. F. Toney, P. L. Geissler, A. P. Alivisatos, *Nano Lett.* **2010**, *10*, 195.
[14] Z. H. Hu, M. D. Fischbein, C. Querner, M. Drndic, *Nano Lett.* **2006**, *6*, 2585.
[15] A. Lutich, L. Carbone, S. Volchek, V. Yakovtseva, V. Sokol, L. Manna, S. Gaponenko, *Phys. Status Solidi RRL* **2009**, *3*, 151.
[16] Y. Huang, C. Y. Chiang, S. K. Lee, Y. Gao, E. L. Hu, J. De Yoreo, A. M. Belcher, *Nano Lett.* **2005**, *5*, 1429.
[17] L. S. Li, A. P. Alivisatos, *Adv. Mater.* **2003**, *15*, 408.
[18] F. Kim, S. Kwan, J. Akana, P. D. Yang, *J. Am. Chem. Soc.* **2001**, *123*, 4360.
[19] Y. Amit, A. Faust, I. Lieberman, L. Yedidya, U. Banin, *Phys. Status Solidi A* **2012**, *209*, 235.
[20] S. Y. Zhang, M. D. Regulacio, M. Y. Han, *Chem. Soc. Rev.* **2014**, *43*, 2301.
[21] a) M. Hasegawa, Y. Hirayama, S. Dertinger, *Appl. Phys. Lett.* **2015**, *106*, 051103; b) T. Aubert, L. Palangetic, M. Mohammadimasoudi, K. Neyts, J. Beeckman, C. Clasen, Z. Hens, *ACS Photonics* **2015**, *2*, 583.
[22] M. Hasegawa, Y. Taira, *J. Photopolym. Sci. Technol.* **1995**, *8*, 241.
[23] S. Martin, S. Klaus, K. Vladimir, C. Vladimir, *Jpn. J. Appl. Phys.* **1992**, *31*, 2155.
[24] K. Ichimura, Y. Suzuki, T. Seki, A. Hosoki, K. Aoki, *Langmuir* **1988**, *4*, 1214.
[25] V. Chigrinov, S. Pikin, A. Verevochnikov, V. Kozenkov, M. Khazimullin, J. Ho, D. D. Huang, H. S. Kwok, *Phys. Rev. E* **2004**, *69*, 061713.
[26] a) T. Du, J. Schneider, A. K. Srivastava, A. S. Susha, V. G. Chigrinov, H. S. Kwok, A. L. Rogach, *ACS Nano* **2015**, *9*, 11049; b) J. Schneider, W. Zhang, A. K. Srivastava, V. G. Chigrinov, H.-S. Kwok, A. L. Rogach, *Nano Lett.* **2017**, *17*, 3133.
[27] a) E. A. Shteyner, A. K. Srivastava, V. G. Chigrinov, H. S. Kwok, A. D. Afanasyev, *Soft Matter* **2013**, *9*, 5160; b) A. D. Kiselev, V. G. Chigrinov, H.-S. Kwok, *Phys. Rev. E* **2009**, *80*, 011706.
[28] L. Carbone, C. Nobile, M. De Giorgi, F. D. Sala, G. Morello, P. Pompa, M. Hytch, E. Snoeck, A. Fiore, I. R. Franchini, M. Nadasan, A. F. Silvestre, L. Chiodo, S. Kudera, R. Cingolani, R. Krahne, L. Manna, *Nano Lett.* **2007**, *7*, 2942.
[29] A. K. Srivastava, W. Hu, V. G. Chigrinov, A. D. Kiselev, Y. Q. Lu, *Appl. Phys. Lett.* **2012**, *101*, 031112.
[30] A. K. Srivastava, X. Q. Wang, S. Q. Gong, D. Shen, Y. Q. Lu, V. G. Chigrinov, H. S. Kwok, *Opt. Lett.* **2015**, *40*, 1643.
[31] V. A. Trofimov, V. R. Yu, *Phys.-Usp.* **1968**, *11*, 276.
[32] J. Planelles, F. Rajadell, J. I. Climente, *J. Phys. Chem. C* **2016**, *120*, 27724.
[33] a) M.-C. Tseng, O. Yaroshchuk, T. Bidna, A. K. Srivastava, V. Chigrinov, H.-S. Kwok, *RSC Adv.* **2016**, *6*, 48181; b) L. Tan, J. Y. Ho, A. K. Srivastava, H. S. Kwok, *IEEE Photonics Technol. Lett.* **2014**, *26*, 1096; c) T. Du, F. Fan, A. K. Srivastava, V. Chigrinov, H.-S. Kwok, *J. Soc. Inf. Disp.* **2014**, *22*, 518.
[34] C. Fernandez-Maloigne, *Advanced Color Image Processing and Analysis*, Springer, New York **2012**.
[35] X. Zhang, H. Lin, H. Huang, C. Reckmeier, Y. Zhang, W. C. Choy, A. L. Rogach, *Nano Lett.* **2016**, *16*, 1415.